Antiproliferative and Apoptotic Effects of the Herbal Agent *Pygeum africanum* on Cultured Prostate Stromal Cells From Patients With Benign Prostatic Hyperplasia (BPH)

Maria T. Quiles,[1]* Maria A. Arbós,[1] Antònia Fraga,[1] Inés M. de Torres,[2] Jaume Reventós,[1] and Juan Morote[3]

[1]*Institut de Recerca, Hospital Universitari Vall d'Hebron, Universitat Autònoma de Barcelona, Barcelona, Spain*
[2]*Department of Pathology, Hospital Universitari Vall d'Hebron, Universitat Autònoma de Barcelona, Barcelona, Spain*
[3]*Department of Urology, Hospital Universitari Vall d'Hebron, Universitat Autònoma de Barcelona, Barcelona, Spain*

BACKGROUND. Previous reports show that the herbal agent *Pygeum africanum* (PA) used to treat benign prostatic hyperplasia (BPH) inhibits proliferation of prostate stromal cells from BPH tissues. To determine underlying mechanisms, we compared proliferative and apoptotic responses to PA between BPH and non-BPH prostate stromal cells with a focus on the specific reaction displayed by stromal cell subsets. An interaction of PA with growth factors and hormones was also investigated.

METHODS. Primary prostate stromal cells from BPH/LUTS patients undergoing open prostatectomy (n = 3) and patients without benign prostatic hyperplasia (BPH) undergoing cystectomy (n = 3) were treated with PA. Cells were characterized by immunofluorescence. Sensitivity to PA was determined using proliferation assays. Apoptosis, transforming growth factor B1 (TGFB1), fibroblast growth factor 2 (FGF2), vimentin, α smooth muscle actin (αSMA), and smoothelin expression were examined after PA treatment. Cell immunophenotype and proliferation were tested after incubating cells with PA plus either FGF2, TGFB1, vascular endothelial growth factor (VEGF), dihydrotestosterone (DHT) or 17β-estradiol (E2).

RESULTS. Antiproliferative potency and apoptosis induced by PA on stromal cells were increased in BPH versus non-BPH cells. Apoptosis targeted αSMA+ cells, more abundant in BPH cells. Downregulation of TGFB1 expression was induced by PA. FGF2 increased cells sensitivity to PA. Incubation with other mitogenic factors like VEGF, DHT, and E2 decreased sensitivity to PA. Both TGFB1 and E2 blocked the antiproliferative activity of PA.

CONCLUSIONS. Results suggest that PA is antiproliferative and apoptotic on proliferative prostate fibroblasts and myofibroblasts but not on smooth muscle cells. Mechanisms of action include TGFB1 downregulation and inhibition of FGF2 specific signaling. *Prostate 70: 1044–1053, 2010.* © 2010 Wiley-Liss, Inc.

KEY WORDS: **myofibroblast; reactive stroma; smooth-muscle cell; phytotherapy; growth factors and hormones**

Additional Supporting Information may be found in the online version of this article.

Maite Quiles and Maria A. Arbós contributed equally to this work.

None of the contributing authors have any conflicts of interest.

Grant sponsor: Elfar-Drag (Madrid, Spain); Grant sponsor: Instituto Carlos III, Ministerio de Ciencia e Innovación, Spain; Grant number: RTICC RD06/0020/0058; Grant sponsor: Departament de Universitats, Recerca i Societat de la Informacio, Generalitat de Catalunya, Spain; Grant number: 2005SGR00553.

*Correspondence to: Maria T. Quiles, PhD, Institut de Recerca, Hospital Universitari Vall d'Hebron, Pg. Vall d'Hebron 119-139, 08035 Barcelona, Spain. E-mail: mtquiles@ir.vhebron.net

Received 20 November 2009; Accepted 6 January 2010
DOI 10.1002/pros.21138
Published online 5 April 2010 in Wiley InterScience (www.interscience.wiley.com).

INTRODUCTION

Symptomatic BPH is an extremely common disorder in men intimately related to ageing. It leads to bladder outlet obstruction associated with lower urinary tract symptoms (LUTS) that reduce the patient's quality of life [1,2]. Troublesome LUTS can occur in up to 30% of men older than 65 years.

The etiology of BPH is not completely understood. The morphometrical predominance of fibromuscular stroma suggests that it is primarily caused by fibrotic changes and an unproportional hyperproliferation of prostate stromal cells (PSC) [3,4]. Among the stromal cell subtypes, activated αSMA+ myofibroblasts prevail in BPH and are the major source of connective tissue [5,6]. Both epithelial–mesenchymal transition and fibroblast-to-myofibroblast transdifferentiation are their potential sources [5,7]. Myofibroblasts contribute to the reactive stroma in BPH with concurrent alterations in cytokines, growth factors, and extracellular matrix components [5].

Phytotherapy is one of the current medical therapies in treating modest-to-severe LUTS associated to BPH. Although controversial, phytotherapy is considered an interesting approach by BPH guidelines [8,9], and it enjoys wide application in Europe and recently in America as well. Its main limitation to be a recommended medical therapy is that only few of the available studies meet the criteria defined in the sixth International Consultation on New Developments in Prostate Cancer and Prostate Disease [10]. Another limitation is that many questions concerning mechanisms of action remain unanswered.

Extract from the bark of the African plum tree, *Pygeum africanum* (PA), is one of the most commonly used drugs in this category. Preliminary results reveal clinical efficacy [11,12]. Its effects have been attributed to its content in phytosterols, pentacyclic triterpenes, and ferulic acid esters. In animal models, PA reverses bladder and prostate symptoms [13,14]. In vitro, it inhibits the growth of a wide variety of cells, including prostate epithelial and stromal cells [15,16]. The putative molecular bases include cell-cycle arrest [17], inhibition of cell signaling pathways at the level of protein kinase C [16–18], apoptosis [18] and binding ability to estrogens and androgen receptors [19].

It was the aim of this study to further explore the mechanisms of action of PA comparing its antiproliferative and apoptotic effects on primary human BPH prostate stromal cells (BPH-PSC) versus non-BPH prostate stromal cells (CTL-PSC) obtained from normal transition zone, with special regard to which stromal cell subtypes were present and whether they had different sensitivity to PA.

MATERIALS AND METHODS

Source of Tissues

Prostate specimens were obtained according to the Internal Review and Ethical Committee of our Institution. Informed written consent was obtained from patients. Transition zone of BPH samples was taken from open prostatectomy specimens ($n = 3$; prostate volume >80 ml). Control non-BPH samples of transition zone were collected from radical cystoprostatectomy specimens ($n = 3$; prostate volume <20 ml) to treat muscle invasive bladder cancer. Patient age was 66.34 ± 3.78 years in BPH patients and 60.34 ± 6.22 years in non-BPH patients. No patient received treatment for LUTS 2 months prior surgery. Serum PSA level was lower than 4 ng/ml. Tissue collection procedure was optimized through culture efficiency tests of prostate explants (explant adhesion and cell growth) and only tissues taken within 30 min of surgery were included in the study. A slice of tissue was embedded in Sakura Tissue-Tek OCT Compound (Sakura Finetek Europe), and stored at -80°C for histology. Another fragment was placed in fresh cell culture medium to subsequent culture.

Cell Culture and Treatments

Primary cultures of PSC were established from fresh tissues according to previously described methods [20]. Cells were grown in RPMI 1640 (Gibco, Invitrogen, Barcelona, Spain) supplemented with 10% heat-inactivated FBS, penicillin (0.1 g/L), streptomycin (0.1 g/L), 2 mM L-glutamine, and 20 mM HEPES (all Gibco) under standard conditions. Detection of epithelial cells was performed with anti pan-keratin antibodies (Keratin, Pan Ab-1 Clone AE1/AE3 mouse mAb; LabVision Corp./Neomarkers, Bionova, Madrid, Spain). Cell cultures were included in the study after histopathological diagnostic confirmation of their matched fresh-frozen tissue (Fig. 1). The six cell lines (three CTL-PSC and three BPH-PSC) were used in each one of the assays. Experiments were carried out between passages 3 and 5.

The PA extract was obtained from Elfar-Drag (Madrid, Spain). It was reconstituted in DMSO to 20 g/L, further heated to 37°C, and sonicated for 30 min. After clearing by centrifugation (10,000*g*, 15 min, 4°C) and filtration (through a 0.2 μm filter), the resulting stock solution was analyzed by gas chromatography-mass spectrometry (Carlo Erba Elemental Analyzer 1108 CHNSO). Consistent with previous reports [21,22], major compounds were β-sitosterol, the monoterpen alcohol α-terpineol, long chain fatty acids (e.g., palmitic acid and stearic acid) and fatty acid esters

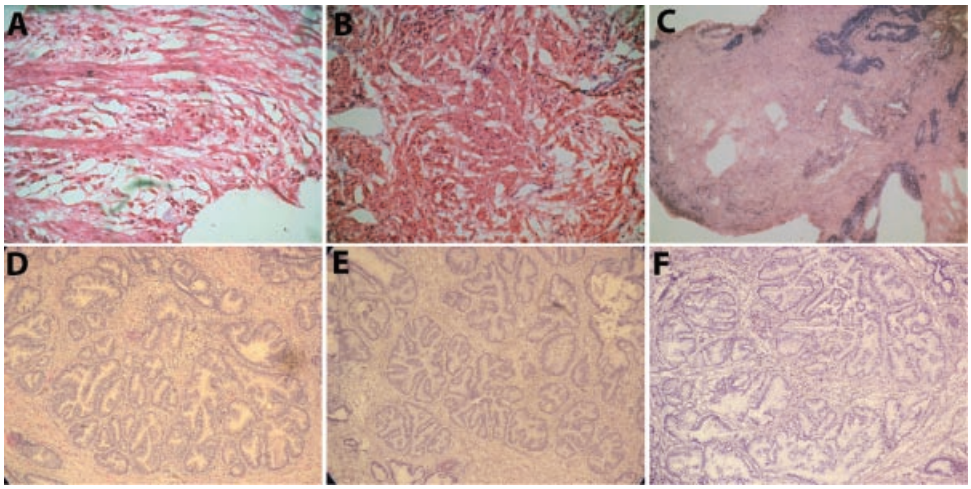

Fig. 1. Histology of prostate tissues before cell culture. Control non-BPH samples (n = 3 patients) of transition zone were collected from radical cystoprostatectomy specimens to treat muscle invasive bladder cancer (**A**–**C**; corresponding to different patients). Transition zone of BPH samples (n = 3) was taken from open prostatectomy specimens (**D**–**F**; corresponding to different patients). Tissues were embedded in Sakura Tissue-Tek OCT Compound, and stored at −80°C for histology. Hematoxylin and eosin staining was performed (magnification 100×). [Color figure can be viewed in the online issue, which is available at www.interscience.wiley.com.]

(Fig. 2). The stock solution was aliquoted and stored at −80°C. The length of exposure times to PA was 24 hr in all the experiments. The final concentration of DMSO in culture medium never exceeded 0.2% (vol/vol), a concentration not deleterious to prostate stromal cells.

Immunofluorescence

Stromal cell subsets were identified by immunofluorescence labeling with cell specific markers. Stromal cells grown on 12-mm round glass cover-slips (20,000 cells/cover-slip) were fixed in 4% paraformaldehyde for 20 min. After washes, cells were permeabilized with 0.5% Triton X-100 in PBS for 10 min, blocked with PBS/2% BSA for 1 hr, and incubated with monoclonal antibodies from Chemicon (Grupo Taper, Madrid, Spain) to vimentin (clone V9; 1:200), αSMA (clone ASM-1; 1:200) or smoothelin (clone R4A; 1:100) for 2 hr. After washing, cover-slips were incubated with secondary antibody (Alexa Fluor® goat anti-mouse; Molecular Probes, Invitrogen; 1:200) for 1 hr. DAPI counterstaining (Vector Laboratories, Atom, Barcelona, Spain) was performed. Slides were observed by confocal laser scanning microscopy and the number of positive-staining cells was evaluated to identify fibroblasts (αSMA−/smoothelin−), myofibroblasts (αSMA+/smoothelin−) and SMC (αSMA+/smoothelin+).

Proliferation Assays

Proliferation assays were performed on cells grown on 24-well plates (20,000 cells/well) with exponentially increasing concentrations of PA (0; 1.78; 3.16; 56.23;

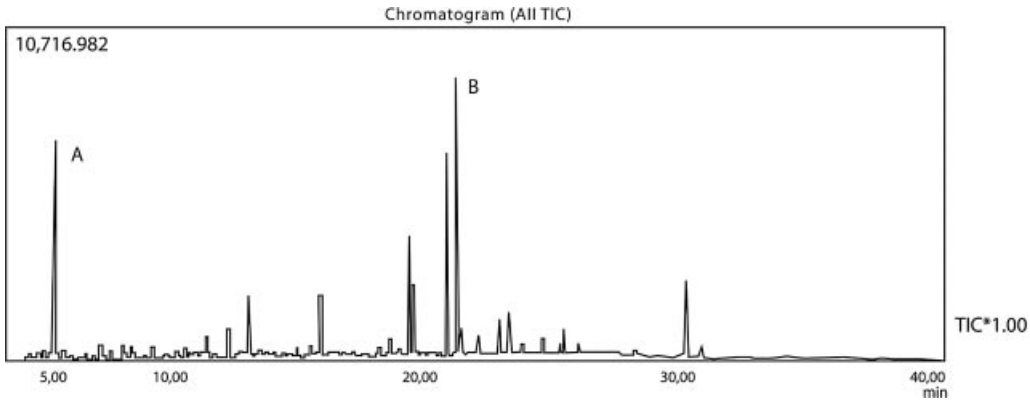

Fig. 2. Gas chromatography-mass spectrometry of *Pygeum africanum* extract. Arrows indicate major compounds α-terpineol (**A**) and β-sitosterol (**B**).

10.00; 17.78; 31.62; and 56.23 μg/ml) for 24 hr. Half maximal effective concentration (EC50) of PA extract was estimated from the resulting dose–response curves for each stromal cell line. Other assays were carried out using PA at its antiproliferative EC50 concentrations with or without fibroblast growth factor 2 (FGF2) (10, 100 ng/ml), transforming growth factor B1 (TGFB1) (1, 10, 100 nM), vascular endothelial growth factor (VEGF) (10, 100 nM), dihydrotestosterone (DHT) (10, 100 nM), and 17β-estradiol (E2) (10, 100 nM). We purchased DHT and E2 from Sigma-Aldrich Química and TGFB1, FGF2, and VEGF from R&D Systems (SG Servicios Hospitalarios, Barcelona, Spain). Cells were pulse labeled for 18 hr with 0.5 μCi of [*methyl*-^{3}H] thymidine/ml (Amersham Pharmacia Biotech, Barcelona, Spain) and washed with PBS, 5% trichloroacetic acid, and 100% ethanol. After air-drying, residues were solubilized in 0.2 N NaOH and neutralized with 0.1 N HCl. Radioactivity was counted with a beta scintillator. For cell proliferation recovery, cells were treated for 24 hr with PA (EC50). Proliferation was determined at 18, 24, 48, and 72 hr, after 18 hr of [*methyl*-^{3}H] thymidine incorporation.

TUNEL Assay

Apoptosis was assessed by the terminal deoxynucleotidyl transferase-mediated dUTP nick end labeling (TUNEL) method on cells grown in glass cover-slips (20,000 cells/cover-slip) treated with either vehicle or PA (EC50) for 24 hr as described. After treatment, cells were analyzed for apoptosis by the TUNEL technique using the In Situ Cell Death Detection kit (Roche Diagnostics, Barcelona, Spain) according to the manufacturer's instructions, followed by embedding in Mowiol 4-88 mounting medium. Cells were visualized using confocal laser scanning microscopy.

RNA Extraction and Semiquantitative RT-PCR

To evaluate vimentin, αSMA, smoothelin, TGFB1 and FGF2 gene expression, total RNA was extracted from 1.5×10^6 cells grown on 10-cm plates and treated with either PA or vehicle as described before (EC50; 24 hr). TRIzol (Invitrogen) was used and total RNA was reverse transcribed using Superscript II reverse transcriptase (Invitrogen) and random hexadeoxynucleotide primers. PCR reactions were run using human-specific primers (Table I) and TaqDNA polymerase (Invitrogen). Ribosomal P19 antigen mRNA served as housekeeping gene. Primers were designed using the free Primer3 software. PCR products were separated on 2% agarose gels, detected with ethidium bromide and quantified by densitometry (Quantity One Software; Bio-Rad). Results were normalized to RP19 antigen RT-PCR.

TABLE I. DNA RT-PCR Primers Used in This Study

RPL19	
Forward	5′-ATCGATCGCCACATGTATCA-3′
Reverse	5′-GCGTGCTTCCTTGGTCTTAG-3′
Vimentin	
Forward	5′-GAGAACTTTGCCGTTGAAGC-3′
Reverse	5′-TCCAGCAGCTTCCTGTAGGT-3′
αSMA	
Forward	5′-ACCCTGGCTTAATATG-3′
Reverse	5′-ACTGGTGTCCATGTGG-3′
Smoothelin	
Forward	5′-CTGGGGATCTCACCAGAAAG-3′
Reverse	5′-GTGCAGTCAATTCCTCCACA-3′
TGFB1	
Forward	5′-GGGACTATCCACCTGCAAGA-3′
Reverse	5′-CCTCCTTGGCGTAGTAGTCG-3′
FGF2	
Forward	5′-GAGAAGAGCGACCCTCACAT-3′
Reverse	5′-ACTGCCCAGTTCGTTTCAGT-3′

Western Blot Analysis

Western blotting was performed with cells grown on 10-cm plates (1.5×10^6 cells) and treated with either PA (EC50) or vehicle for 24 hr as described before. Cell lysis was carried out in cold RIPA buffer (50 mM Tris–HCl pH 7.6, 150 mM NaCl, 1 mM EDTA, 0.25% sodium deoxycolate, 1% Triton X-100, 0.1% SDS) containing protease inhibitors (Calbiochem). Cytosolic proteins were extracted using Calbiochem Proteo Extract kit following the manufacturer's protocol. Total proteins were quantified using the Bio-Rad Protein Assay. Equal amounts of protein were subjected to SDS–PAGE and transferred onto nitrocellulose membrane. The membrane was incubated overnight at 4°C with primary antibodies to vimentin (clone V9, 1:1,000), αSMA (clone ASM-1; 1:1,000) and smoothelin (clone R4A; 1:100), followed by incubation with horseradish peroxidase-conjugated secondary antibody. Immunoreactive proteins were detected using enhanced chemiluminescence (Amersham Pharmacia Biotech). Silver-stained SDS–PAGE gels were used as loading controls. Analysis was performed using Quantity One Software.

Statistical Analysis

Statistical analysis was achieved using Prism software (ver. 3.02 for Windows; GraphPad Software, Inc.). Dose–response curves were fitted to Hill equation in nonlinear regression analyses. Differences in half-maximal stimulatory values (EC50) of treated BPH-PSC and CTL-PSC were tested for statistical significance by the unpaired Student's *t*-test. Statistical analyses were performed by Student's *t*-tests and

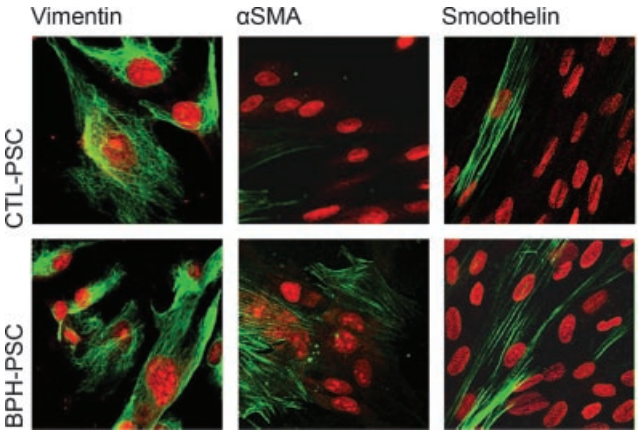

Fig. 3. Stromal cell subsets identification. Representative micrograph showing immunofluorescence in PSC cultures established from fresh tissues. Cells were stained for vimentin (400×), αSMA (200×), and smoothelin (200×), visualized by green fluorescence. Nuclei were counterstained in red by DAPI. Vimentin staining was detected in 100% of the cells. [Color figure can be viewed in the online issue, which is available at www.interscience.wiley.com.]

two-way ANOVA (group × treatment). Probability values of less than 0.05 indicated a significant difference.

RESULTS

Identification of PSC Subtypes

Vimentin expression was observed in 100% of the cells (Fig. 3). Contaminating epithelial cells were ruled out by the absence of cytokeratin detection. Table II shows that immunofluorescent detection of αSMA was found in 25% of BPH-PSC compared to 9% in CTL-PSC ($P = 0.02$). Smoothelin positive cells were slightly increased in BPH-PSC compared to CTL-PSC (17% vs. 11%; $P = 0.05$).

Effects of PA Treatment

Figure 4A illustrates that PA dose dependently decreased cell proliferation with enhanced potency in BPH-PSC as compared to CTL-PSC (EC50 = 7.35 μg/ml vs. 18.68 μg/ml; $P = 0.03$). Maximal PA effect was similar in BPH and CTL-PSC cultures. After withdrawal of PA, the abrogated cell proliferation recovered in all cell lines in a time-dependent manner (Fig. 4B). BPH-PSC required 6 days to regain their growth while CTL-PSC totally recovered within 4 days. When the stromal cell subsets were evaluated, we verified that the number of αSMA positive cells decreased almost threefold in BPH-PSC, while they were almost unchanged in CTL-PSC (Fig. 5A). Smoothelin positive cells were resistant to PA in both groups. Figure 5B,C shows downregulation of vimentin and αSMA mRNA and protein expression in BPH-PSC after PA treatments, while smoothelin even increased its protein expression. A sevenfold ($P = 0.03$) decrease of TGFB1 mRNA was detected in BPH-PSC (Fig. 5B). According to these results, it was also confirmed that PA induced apoptosis in all stromal cells. More TUNEL positive cells were detected in BPH-PSC than in CTL-PSC (34%; $P = 0.01$). Co-localization experiments showed TUNEL positive nuclei in αSMA positive cells (Fig. 6).

Antiproliferative Effects of PA in Growth Factor and Hormone-Treated PSC

Both FGF2 and VEGF promoted fibroblastic phenotype, that is, spindle morphology and low αSMA and smoothelin cell staining (Fig. 7) in PSC. Treatments with PA hindered VEGF and FGF2-induced cell proliferation (33–38%, 60–65%, respectively), with independence of the group and growth factor concentration (Fig. 8A,B). Treatments with TGFB1 revealed high αSMA and smoothelin immunofluorescent staining in all cells (Fig. 7) and cell growth arrest (Fig. 8C). After PA, cell morphology (data not shown) and antiproliferative activity remained almost unaltered (Fig. 8C). DHT induced stimulatory effects on cell proliferation in a dose-dependent manner in all PSC (Figs. 7 and 8D), that PA was able to change, especially at DHT 100 nM (42–45%; Fig. 8D). Pavement-like appearance was exhibited by cells treated with E2, as well as increased αSMA and smoothelin detection (Fig. 7). At its highest concentration (100 nM), E2 inhibited cell proliferation and cell sensitivity to PA (Fig. 8E).

TABLE II. Prostate Stromal Cell Characterization

	CTL1	CTL2	CTL3	BPH1	BPH2	BPH3
Cell numbera	217 ± 12	205 ± 9	224 ± 8	274 ± 9	263 ± 13	282 ± 10
% αSMA + cells	8.68 ± 6.43	8.80 ± 7.12	10.51 ± 6.60	27.57 ± 8.21	25.24 ± 7.72	22.11 ± 3.44
% Smoothelin + cells	10.31 ± 7.80	8.36 ± 9.81	13.59 ± 6.01	17.56 ± 5.66	18.78 ± 6.33	14.16 ± 7.77

Total cell number (nuclei), αSMA and smoothelin-positive cells were counted from 20 fields (200×) for each stromal cell line. Values are means of two manual cell counts ± SD.

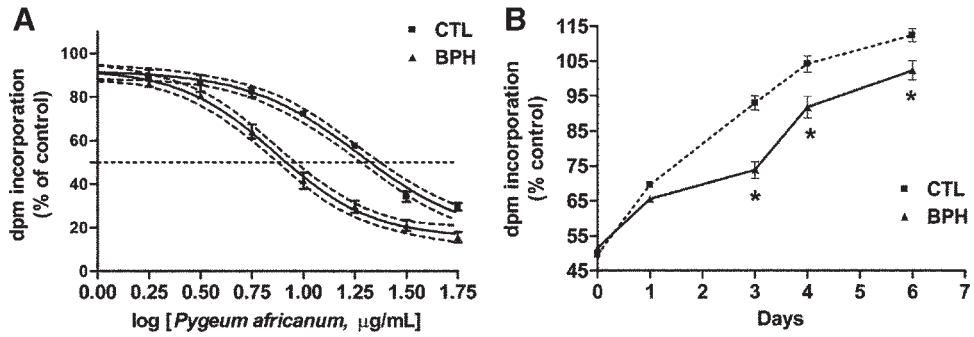

Fig. 4. Effects of PA on cell proliferation. **A**: Dose–response curve for PA inhibition of [*methyl*-^{3}H] thymidine cell incorporation. Stromal cells were incubated with increasing concentrations of PA for 24 hr. The percent of [*methyl*-^{3}H] thymidine (0.5 μCi/ml; 18 hr) incorporated relative to control untreated cells was measured. Dotted line indicates half maximal effect of PA extract. Dotted line crosses dose–response curves at EC50 (half maximal effective concentration). Values are means ± SD. **B**: Time-dependent recovery of cell proliferation after withdrawal of PA (24-hr pretreatment; EC50 dose) from cell media. Proliferation was determined by [*methyl*-^{3}H] thymidine incorporation. Values are means ± SD.

DISCUSSION

Prior to our experiments, we analyzed the phenotype of cultured stromal cells from BPH tissues and compared them with the stromal cell cultures generated from non-BPH transition zone. Immunophenotypic characterization of BPH-PSC indicated the presence of SMC, fibroblasts and myofibroblasts. All three subtypes have been detected before in BPH-PSC with variability in the relative amounts [16,23,24]. In general, SMC biomarkers decrease or even become undetectable in cultured BPH-PSC because of the expansion of pathologically hyperproliferative fibroblasts and myofibroblasts [24]. In CTL-PSC, the number of αSMA and smoothelin positive cells was similar (about 15%), indicating that they were SMC (αSMA+/smoothelin+). This result also suggested that myofibroblasts (αSMA+/smoothelin−) were absent in CTL-PSC, and that fibroblasts were the predominant cells. Thus, myofibroblasts appeared restricted to BPH-PSC cultures. This is consistent with data obtained from human prostates, where smooth muscle prevails in normal transition zone whereas it is replaced by an expansion of myofibroblasts in BPH lesions [5]. Benign prostate hyperplasia involves a phenotypic shift to reactive stroma, similar to wound repair stroma [5,25]. It develops matrix remodeling, extracellular matrix deposition, and growth factor expression and it is composed primarily of myofibroblasts [5,6].

Our laboratory and others have shown that PA inhibits proliferation in cells of different origins [16,17,19,26,27], including human BPH fibroblasts and myofibroblasts [16]. Now we show that PA inhibited cell growth more potently in BPH-PSC than in CTL-PSC, in a dose dependent and reversible fashion. Furthermore, the amount of αSMA+ cells decreased while smoothelin+ cells remained constant after PA treatment in BPH stromal cell cultures. Western blot and RT-PCR confirmed these results, which showed in PA-treated cells an increase in the smoothelin protein band that was due to the smoothelin+ cell resistance to the agent.

Following this line of evidences, double-staining assays indicated that apoptosis induction, with the highest rates in BPH-PSC, was specifically affecting αSMA positive cells. Taken together, our findings support that proliferative fibroblasts and myofibroblasts from BPH tissues are a direct target of PA action, while SMC are resistant to its effects. Apoptosis appeared to be one of the activated mechanisms by PA. Interestingly, in castrated/testosterone-replaced rats, PA treatment prevents cell proliferation but it does not induce modifications in quiescent non-proliferating prostates [18]. Consequently, a link between PA action and cell proliferation status has been proposed [18].

The myofibroblast-based reactive stroma is also present in well-differentiated prostate cancer foci [25]. Therefore, if PA targets reactive cells it should be active against reactive stroma in cancer too. However, it has not been explored weather PA affects prostate cancer stromal cells. Actually, PA has been studied extensively as a therapy for men with BPH but not in men with prostate cancer. In light of our results, it may be concluded that PA might be beneficial in prostate cancer therapeutics as a chemopreventive agent [28]. In fact, antitumoral effects have been described by targeting myofibroblasts in animal models [29], suggesting that even greater effects might be achieved by fostering synergy with other targets.

Data on TGFB1 expression were not quantitative, since they were obtained by conventional RT-PCR. Decrease in TGFB1 expression was consistent with the depletion of myofibroblasts induced by PA, since these

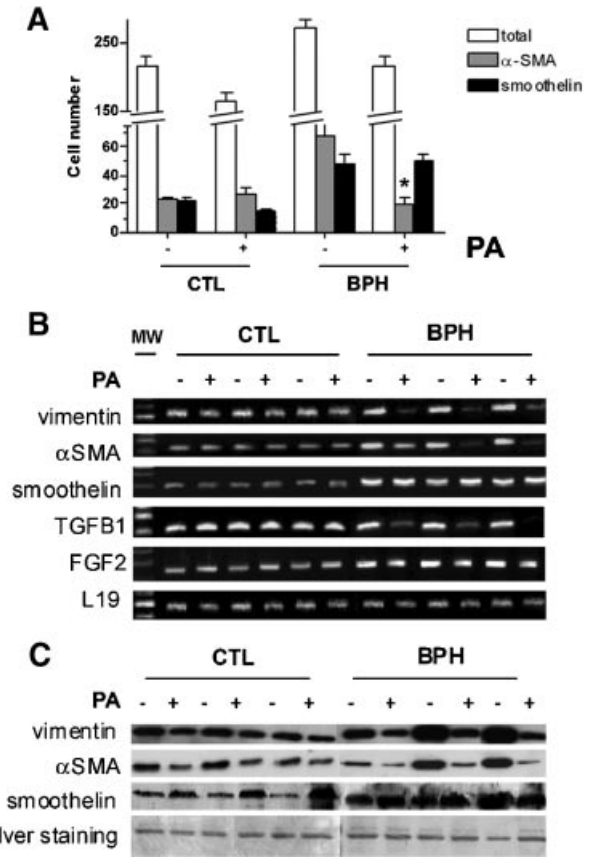

Fig. 5. Selective effects of PA on αSMA positive cells. **A**: Absolute number of total, αSMA and smoothelin-positive cells in PSC cultures after PA treatment. Cells were grown on glass cover-slips (20,000 cells/cover-slip) and treated with PA (EC50) for 24 hr. Immunofluorescent staining of αSMA and smoothelin was performed as explained above. Total cell number (nuclei), αSMA and smoothelin-positive cells were counted from 20 fields (200×) for each stromal cell line. Values are means of three cell cultures ± SD; $^{*}P < 0.05$. **B**: Vimentin, αSMA, smoothelin, TGFBI, and FGF2 mRNA expression in stromal cells after PA treatment (EC50; 24 hr) measured by RT-PCR. RPLI9 was used as a housekeeping gene. Each lane corresponds to one stromal cell line (one patient). **C**: Vimentin, αSMA and smoothelin protein expression in prostate stromal cells measured by Western blot after PA treatment (EC50; 24 hr). Silver-stained gels were used as loading controls. Each lane is one stromal cell line.

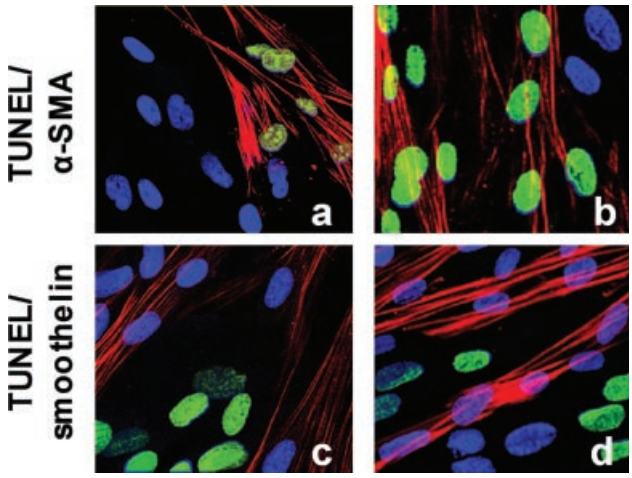

Fig. 6. PA induces apoptosis in αSMA positive prostate stromal cells. Stromal cells (20,000 cells/cover-slip) were subjected to TUNEL (green) combined with αSMA and smoothelin (red) immunofluorescent cell staining after PA treatment for 24 hr (EC50). Non-apoptotic nuclei were stained by DAPI (blue). In the figure, representative micrographs illustrate that only αSMA positive cells showed positive TUNEL nuclei both in CTL-PSC (**a**) and BPH-PSC (**b**). Neither CTL-PSC (**c**) nor BPH-PSC (**d**) cultures showed evidence of apoptosis in its smoothelin positive cells. [Color figure can be viewed in the online issue, which is available at www.interscience.wiley.com.]

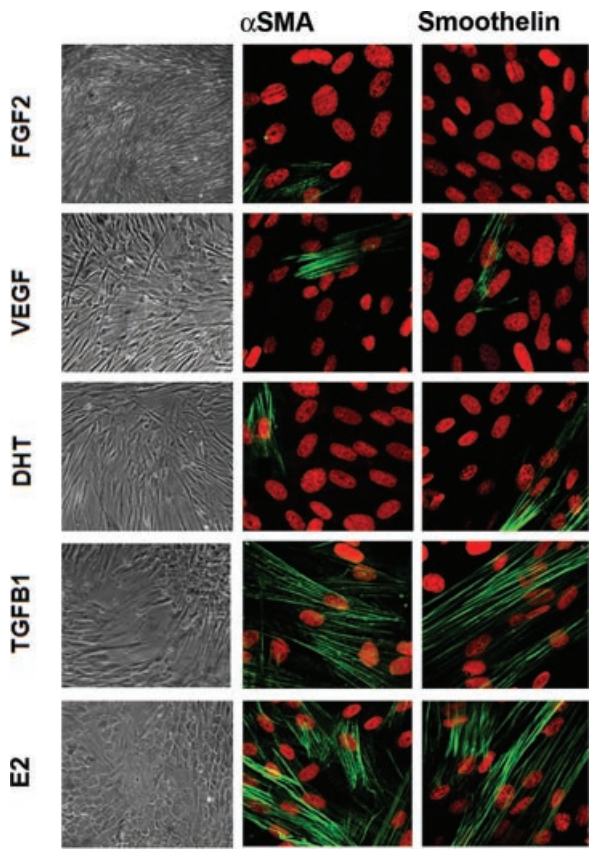

Fig. 7. Morphology, αSMA, and smoothelin expression in prostate stromal cells treated with growth factors and hormones. Prostate stromal cells were incubated with FGF2, VEGF, DHT, TGFBI, and E2 for 72 hr. Cells were subjected to immunofluorescent staining for αSMA, smoothelin (green), and DAPI (red). Representative phase contrast (40×) and fluorescence (200×) photomicrographs for BPH stromal cells are shown. Both FGF2 and VEGF promoted spindle morphology and decreased αSMA and smoothelin cell staining. Conversely, TGFBI and E2 strongly induced αSMA and smoothelin immunofluorescent staining in all cells. [Color figure can be viewed in the online issue, which is available at www.interscience.wiley.com.]

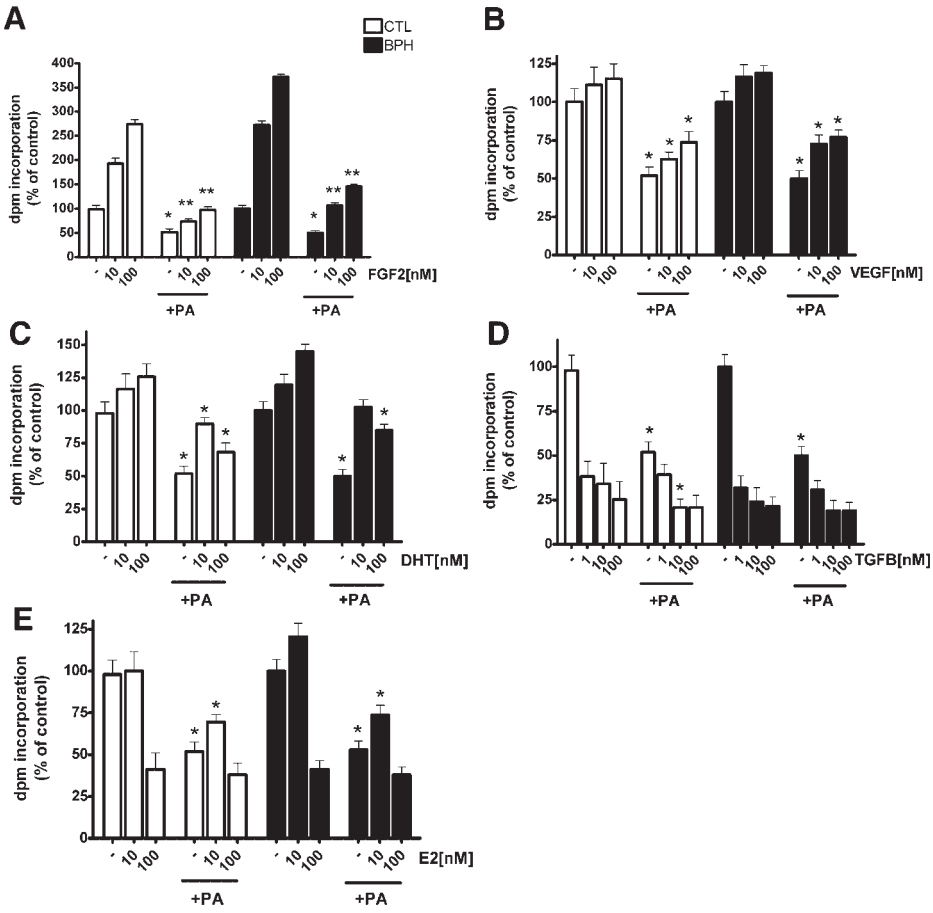

Fig. 8. Cell proliferation changes induced by 72 hr incubations with FGF2 (**A**), VEGF (**B**), DHT (**C**), TGFBI (**D**), and E2 (**E**) in PA-treated and non-treated prostatic stromal cells for the last 24 hr. Cell proliferation was measured by [*methyl*-^{3}H] thymidine incorporation. Values are % relative to non-treated cells and represent mean ± SD. Differences between non-treated and treated cells were studied (*$P < 0.05$; **$P < 0.01$).

stromal cells are the principal source of TGFB in prostatic stroma [30]. Given that this cytokine stimulates fibroblast-to-myofibroblast transdifferentiation and activation, as well as the induction of extracellular matrix protein [31], it may be suggested that PA targeted myofibroblasts not only directly but also indirectly via downregulation of TGFB1 expression. Taken together, our results strongly suggest that the phenotypic features of prostate stromal cells might determine their sensitivity to PA.

P. africanum has many components: phytosterols, pentacyclic triterpenes, ferulic esters, fatty acids, etc. Each of these components has its own mode of action. For this reason, the molecular mechanisms underlying the cell growth inhibitory action of PA are little known. Evidences indicate that prostate stromal cell proliferation induced by EGF, FGF2, and IGF-I as well as protein kinase C activators is inhibited by PA in rats and humans [16,17,27]. Furthermore, it has been suggested that a locus common to the three growth factors is affected via a site that converge near the level of protein kinase C [32,33]. We observed that PA strongly inhibited FGF2-induced cell proliferation in BPH and non-BPH stromal cells. However, cells treated with other mitogenic factors, like VEGF, DHT, and E2 at low concentration, displayed partial resistance to PA action compared to untreated cells. It could be speculated that under the effect of these factors, PA only inhibits those downstream effectors that they have in common with FGF2, like protein kinase C [34,35], and therefore it partially loses its potency. Thus, it is not just the proliferative status but which proliferative mechanisms are induced what may determine PA activity.

The inhibition of protein kinase C may in part contribute to the apoptotic effect of PA in prostate stromal cells. Shenouda et al. [19] have reported that protein kinase C activity inhibition contributes to the apoptotic induction of PA in prostate cancer cells LNCaP and PC3. It is now evident that some signal transduction pathways are common to stimuli that lead to mitogenic and apoptotic responses. Some of the

protein kinases pathways lead to the induction of genes involved in the process of cell proliferation or cell death [36].

Consistent with the apoptotic resistance to PA observed in the smoothelin positive stromal cells, TGFB and high concentrations of E2-induced resistance to PA. Both factors stimulated smoothelin expression in prostate stromal cells. Additionally, neither morphology nor proliferation was altered by PA in these cells. To our knowledge, there are no reports about a protective role of TGFB and E2 against PA. However, it is interesting to note that TGFB downregulates FGF2 signaling and promotes resistance to apoptosis in human myofibroblasts [37]. In rat prostatic stromal cells, the cellular response to E2 is mediated by TGFB [38] and has the potential to oppose apoptosis [39].

CONCLUSIONS

We have attempted to gain insight into the mechanisms underlying the growth inhibitory effects of PA on prostate stromal cells. We provide evidence that PA inhibits cell proliferation and enhances apoptotic cell death of prostate stromal cells, specifically targeting fibroblasts and myofibroblasts. Interestingly myofibroblasts play a major role in BPH progression, when they proliferate and increase their number [5–7]. In this regard, incubation with growth factors and hormones confirmed the link between PA action and the proliferative status of cells mediated by blocking specific mechanisms linked to FGF2 activity. Moreover, cultured differentiated smooth muscle cells were resistant to PA effects.

While caution should be applied when trying to extrapolate our results to human prostate biology due to the use of cultured stromal cells, our observations support the notion that different stromal cell subtypes contribute to BPH having a major impact in its response to PA therapy and conditioning the time at which PA therapy should be initiated. Further studies will be needed to confirm these observations, especially when BPH implies a maturational process of nodular stromal proliferates from fibroblastic and fibromuscular to smooth-muscular nodules [40].

ACKNOWLEDGMENTS

We thank members of the Biomedical Research Laboratory (Institut de Recerca-Hospital Universitari Vall d'Hebron) for their comments, and J Guillén-Martí for critiquing the manuscript. This work was supported by grants made available from Elfar-Drag (Madrid, Spain); Instituto Carlos III, Ministerio de Ciencia e Innovación, Spain (RTICC RD06/0020/0058), and Departament de Universitats, Recerca i Societat de la Informacio, Generalitat de Catalunya, Spain (2005SGR00553).

REFERENCES

1. Berry SJ, Coffey DS, Walsh PC, Ewing LL. The development of human benign prostatic hyperplasia with age. J Urol 1984; 132:474–479.
2. McVary KT. BPH: Epidemiology and comorbidities. Am J Manag Care 2006;12:S122–S128.
3. McNeal JE. Pathology of benign prostatic hyperplasia: Insight into etiology. Urol Clin North Am 1990;17:477–486.
4. Chagas MA, Babinski MA, Costa WS, Sampaio FJB. Stromal and acinar components of the transition zone in normal and hyperplastic human prostate. BJU Int 2002;89:699–702.
5. Schauer IG, Ressler SJ, Tuxhorn JA, Dang TD, Rowley DR. Elevated epithelial expression of interleukin-8 correlates with myofibroblast reactive stroma in benign prostatic hyperplasia. Urology 2008;72:205–213.
6. Schauer IG, Ressler SJ, Rowley DR. Keratinocyte-derived chemokine induces prostate epithelial hyperplasia and reactive stroma in a novel transgenic mouse model. Prostate 2009;69:373–384.
7. Alonso-Magdalena P, Brössner C, Reiner A, Cheng G, Sugiyama N, Warner M, Gustafsson JA. A role for epithelial-mesenchymal transition in the etiology of benign prostatic hyperplasia. Proc Natl Acad Sci 2009;106:2859–2863.
8. Madersbacher S, Alivizatos G, Nordling J, Sanz C, Emberton M, de la Rosette J. EAU 2004 Guidelines on Assessment, Therapy and Follow-Up of Men with Lower Urinary Tract Symptoms Suggestive of Benign Prostatic Obstruction (BPH Guidelines). Eur Urol 2004;46:547–554.
9. Kaplan SA. Update on the American Urological Association guidelines for the treatment of benign prostatic hyperplasia. Rev Urol 2006;8:S11–S17.
10. Abrams P, Chapple C, Khoury S, Roehrborn C, de la Rosette J, International Scientific Committee. Evaluation and treatment of lower urinary tract symptoms in older men. J Urol 2009;181: 1779–1787.
11. Ishani A, MacDonald R, Nelson D, Rutks I, Wilt TJ. *Pygeum africanum* for the tratment of patients with benign prostatic hyperplasia: A systematic review and quantitative meta-analysis. Am J Med 2000;109:654–664.
12. Hutchison A, Farmer R, Verhamme K, Berges R, Navarrete RV. The efficacy of drugs for the treatment of LUTS/BPH, a study in 6 European countries. Eur Urol 2007;51:207–215.
13. Choo MS, Bellamy F, Constantinou CE. Functional evaluation of Tadenan on micturition and experimental prostate growth induced with exogenous dihydrosterone. Urology 2000;55: 192–298.
14. Levin RM, Hass MA, Bellamy F, Horan P, Whitbeck K, Chow PH, Kung LS, Gosling J. Effect of oral Tadenan treatment on rabbit bladder structure and function after partial outlet obstruction. J Urol 2002;167:2253–2259.
15. Yoshimura Y, Yamaguchi O, Bellamy F, Constantinou CE. Effect of *Pygeum africanum* tadenan on micturition and prostate growth of the rat secondary to coadministered treatment and post-treatment with dihydrotestosterone. Urology 2003;61:474–478.
16. Boulbès D, Soustelle L, Costa P, Haddoum M, Bali JP, Hollande F, Magous R. Pygeum africanum extract inhibits proliferation of human cultured prostatic fibroblasts and myofibroblasts. BJU 2006;98:1106–1113.

17. Yablonsky F, Nicolas V, Rifaud JP, Bellamy M. Antiproliferative effect of *Pygeum africanum* extract on rat prostatic fibroblasts. J Urol 1997;157:2381–2387.
18. Solano RM, García-Fernández MO, Clemente C, Querol M, Bellamy F, Sanchez-Chapado M, Prieto JC, Carmena MJ. Effects of *Pygeum africanum* extract (Tadenan) on vasoactive intestinal peptide receptors, G proteins, and adenylyl cyclase in rat ventral prostate. Prostate 2000;45:245–252.
19. Shenouda NS, Sakla MS, Newton LG, Besch-Williford C, Greenberg NM, MacDonald RS, Lubahn DB. Phytosterol *Pygeum africanum* regulates prostate cancer in vitro and in vivo. Endocrine 2007;31:72–81.
20. Jones GE, Wise CJ. Establishment, maintenance, and cloning of human dermal fibroblasts. In: Pollard J, Walker JM, editors. Basic cell culture protocols, series: Methods in molecular biology, Vol. 75, 2nd edition, London, UK: Humana Press; 1997. pp 13–21.
21. Ganzera M, Croom EM, Khan IA. Determination of the fatty acid content of pumpkin seed, Pygeum and saw palmetto. J Med Food 1999;2(1):21–27.
22. Gathumbi PK, Mwangi JW, Mugera GM, Njiro SM. Toxicity of chloroform extract of *Prunus africana* stem bark in rats: Gross and histological lesions. Phytother Res 2002;16:244–247.
23. Fry PM, Hudson DL, O'Hare MJ, Masters JR. Comparison of marker protein expression in benign prostatic hyperplasia in vivo and in vitro. BJU Int 2000(5):504–513.
24. Lin VK, Wang SY, Vázquez DV, Xu CC, Zhang S, Tang L. Prostatic stromal cells derived from benign prostatic hyperplasia specimens possess stem cell like property. Prostate 2007(67): 1265–1276.
25. Tuxhorn JA, Ayala GE, Smith MJ, Smith VC, Dang TD, Rowley DR. Reactive stroma in human prostate cancer: Induction of myofibroblast phenotype and extracellular matrix remodeling. Clin Cancer Res 2002;8: 2912–2923.
26. SantaMaría A, Paciucci R, Reventós J, Morote J, Thomson TM. Antimitogenic effect of *Pygeum africanum* extracts on human prostatic cancer cell lines and explants from benign prostatic hyperplasia. Arch Esp Urol 2003;56:369–378.
27. Paubert-Braquet M, Montboisse JC, Biochot-Lagente E, Servent-Saez N, Serikoff A, Cavé A, Hocquemiller R, Dupont C, Fourneau C, Borel JP. Inhibition of bFGF and EGF-induced proliferation of 3T3 fibroblasts by extract of *Pygeum africanum* (Tadenan). Biomed Pharmacother 1994;48:43s–47s.
28. Yarnell E, Abascal K. Holistic approaches to prostate cancer. Altern Complement Ther 2008;14(4):164–180.
29. Sheffer Y, Leon O, Pinthus JH, Nagler A, Mor Y, Genin O, Iluz M, Kawada N, Yoshizato K, Pines M. Inhibition of fibroblast to myofibroblast transition by halofuginone contributes to the chemotherapy-mediated antitumoral effect. Mol Cancer Ther 2007;6(2):570–577.
30. Lucia MS, Lambert JR. Growth factors in benign prostatic hyperplasia: Basic science implications. Curr Urol Rep 2008; 9(4):272–278.
31. Untergasser G, Gander R, Lilg C, Lepperdinger G, Plas E, Berger P. Profiling molecular targets of TGF-beta1 in prostate fibroblast-to-myofibroblast transdifferentiation. Mech Ageing Dev 2005; 126:59–69.
32. Levin RM, Das AK. A scientific basis for the therapeutic effects of Pygeum africanum and Serenoa repens. Urol Res 2000;28:201–209.
33. Edgar AD, Levin R, Constantinou CE, Denis L. A critical review of the pharmacology of the plant extract of Pygeum africanum in the treatment of LUTS. Neurourol Urodyn 2007;26:458–463.
34. Reynolds AR, Kyprianou N. Growth factor signalling in prostatic growth: Significance in tumour development and therapeutic targeting. Br J Pharmacol 2006;147:S144–S152.
35. Zhu ML, Kyprianou N. Androgen receptor and growth factor signaling cross-talk in prostate cancer cells. Endocr Relat Cancer 2008;15(4):841–849.
36. Maroni PD, Koul S, Meacham RB, Koul HK. Mitogen activated protein kinase signal transduction pathways in the prostate. Cell Commun Signal 2004;2(1):5.
37. Chambers RC, Leoni P, Kaminski N, Laurent GJ, Heller RA. Global expression profiling of fibroblast responses to transforming growth factor-beta 1 reveals the induction of inhibitor of differentiation-1 and provides evidence of smooth muscle cell phenotypic switching. Am J Pathol 2003;162:533–546.
38. Hong JH, Song C, Shin Y, Kim H, Cho SP, Kim WJ, Ahn H. Estrogen Induction of smooth muscle differentiation of human prostatic stromal cells is mediated by transforming growth factor-beta. J Urol 2004;171:1965–1969.
39. Luo Y, Waladali W, Li S, Zheng X, Hu L, Zheng H, Hu W, Chen C. 17beta-estradiol affects proliferation and poptosis of rat prostatic smooth muscle cells by modulating cell cycle transition and related proteins. Cell Biol Int 2008;32:899–905.
40. Bierhoff E, Vogel J, Benz M, Giefer T, Wernert N, Pfeifer U. Stromal nodules in benign prostatic hyperplasia. Eur Urol 1996; 29:345–354.